SiO_yN_x/SiN_x stack: A promising surface passivation layer for high-efficiency and potential-induced degradation resistant mc-silicon solar cells

Chunlan Zhou[1*], Junjie Zhu[2*], Su Zhou[1], Yehua Tang[3], Sean E. Foss[2], Halvard Haug[2], Ørnulf Nordseth[2], Erik S. Marstein[2], Wenjing Wang[1]

1, The Key Laboratory of Solar Thermal Energy and Photovoltaic System, Institute of Electrical Engineering, Chinese Academy of Science, Beijing, China

2, Solar Energy Department, Institute for Energy Technology, Instituttveien 18, 2007 Kjeller, Norway

3,. Eoplly New Energy Technology Co., Ltd, Nantong 226000, China

ABSTRACT

A thin SiO_yN_x film was inserted below a conventional SiN_x antireflection coating used in c-Si solar cells in order to improve the surface passivation and the solar cell's resistance to potential-induced degradation (PID). The effect of varying the flow ratio of the N_2O and SiH_4 precursors and the deposition temperature for the SiO_yN_x thin film upon material properties were systematically investigated. An excellent surface passivation was obtained on FZ p-type polished silicon wafers, with the best results obtained with a SiO_yN_x film deposited at a very low temperature of 130 ◦C and with an optical refractive index of 1.8. In the SiO_yN_x/SiN_x stack structure, a SiO_yN_x film with ~6 nm thickness is sufficient to provide excellent surface passivation with an effective surface recombination velocity S_{eff} < 2 cm/s. Furthermore, we applied the optimized SiO_yN_x/SiN_x stack on multicrystalline Si solar cells as a surface passivation and antireflection coating, resulting in a 0.5% absolute average conversion efficiency gain compared to that of reference cells with conventional SiN_x coating. Moreover, the cells with the SiO_yN_x/SiN_x stack layers show a significant increase in their resistance to PID. Nearly zero degradation in shunt resistance was obtained after 24 hours in a PID test, while a single SiN_x-coated silicon solar cell showed almost 50% degradation after 24 hours.

KEYWORDS

SiO_yN_x/SiN_x stack; silicon solar cell; surface passivation; high efficiency; potential induced degradation

*Correspondence

Chunlan Zhou, The Key Laboratory of Solar Thermal Energy and Photovoltaic System, Institute of Electrical Engineering, Chinese Academy of Science, Beijing, 100190, China

E-mail: zhouchl@mail.iee.ac,cn

Junjie Zhu, Solar Energy Department, Institute for Energy Technology, Instituttveien 18, 2007 Kjeller, Norway

E-Mail: junjie.zhu@ife.no

1. INTRODUCTION

Amorphous, hydrogenated silicon oxynitride (SiO_yN_x:H) prepared by plasma-enhanced chemical vapor deposition (PECVD) can exhibit low absorbance and an adjustable refractive index between 1.45 and 1.9 [1] depending on its composition. Considerable focus has been placed on developing SiO_yN_x as surface passivation and antireflection coatings (ARC) for thin crystalline Si solar cells [2]. Double layer stacks of amorphous SiO_yN_x and silicon nitride (SiN_x) have also attracted significant interest for Si solar cell application, since such stacks can provide a high positive fixed charge density (Q_f) on the order of 10^{12} cm^{-2}, which is sufficient for field effect passivation of both p and n-type Si surfaces [3].

For surface passivation layers used in silicon solar cells, passivation quality as well as its thermal stability are important issues [4, 5]. An industrially feasible double-layer stack comprised of a thin, silicon-rich SiO_yN_x layer and a conventional SiN_x layer has previously been shown to exhibit greatly improved passivation after a high-temperature annealing step [4]. However, in some cases the passivation quality of stacks containing Si-rich SiO_yN_x layers has also been observed to degrade significantly after firing [5]. Hallam et al. [6] presented a quantitative analysis of the relationship between the composition of PECVD SiO_yN_x films and surface passivation on float zone (FZ) silicon wafers with non-diffused planar surfaces. They achieved the best effective carrier lifetime (τ_{eff}) of 1.8 ms on n-type and 1.1 ms on p-type Si. A conversion efficiency of 16.8% was obtained on an 18 μm thick silicon solar cell using PECVD SiO_yN_x films as the ARC [7]. However, their metallization process was kept at low temperature below 450 °C, indicating that the SiO_yN_x films lacked high temperature stability. To our knowledge, a detailed study of the application of the SiO_yN_x/SiN_x stacks in industrial crystalline silicon solar cells has not been reported yet. Our previous studies have shown that a SiO_yN_x/SiN_x stack has a potential as ARC for Si solar cells due to good surface passivation, thermal stability and resistance to potential-induced degradation (PID) [8]. In this structure, SiO_yN_x was used as a surface passivation layer on the Si substrate, and the capping layer of SiN_x was used as a source of hydrogen which diffuses through the SiO_yN_x films to

passivate the structure defect in dielectric films and at the interface between SiO_yN_x films and Si. At the same time, the SiO_yN_x layers together with the silicon nitride layer meets the requirement to a λ / 4 anti-reflection coating. So optimum surface passivation and optical properties for SiO_yN_x for silicon solar cell application are very important. In this paper, we further investigate the use of SiO_yN_x/SiN_x stacks for Si solar cell applications. The effect of the SiO_yN_x deposition conditions on the film composition as well as the surface passivation quality of the stack is systematically investigated. Industrial multicrystalline silicon (mc-Si) solar cells with a SiO_yN_x/SiN_x stack are fabricated, and solar cell performance and PID measured. Finally, the mechanisms responsible for the improved device performance due to the incorporation of the SiO_yN_x/SiN_x stack is discussed.

2. EXPERIMENTAL DETAILS

SiO_yN_x layers were deposited by PECVD (PlasmaLab System 133, Oxford Instruments) with pure silane (SiH_4) and nitrous oxide (N_2O) as precursors. The deposition pressure and plasma power were fixed at 500 mTorr and 58 mW/cm^2, respectively. The capping SiN_x layers and single SiN_x film as reference were deposited with the same equipment using NH_3 and SiH_4 at standard process for silicon surface passivation [9]: a deposition temperature of 400 °C and plasma power of 47 mW/cm^2 at pressure of 800 mTorr. The optical refractive index (n) of the resulting SiN_x films was 2.04. For all samples, the wavelength-dependent refractive index, n (λ), and the thickness of deposited films, were deduced by spectroscopic ellipsometry (WVASE32, J. A. Woollam Co. Inc). The value of n at λ = 630 nm was used to estimate the optical properties of the different films.

1–3 Ω·cm 4 " p-type polished FZ Si wafers with a bulk minority carrier lifetime of at least 3 ms were used as substrates for Fourier transform infrared spectroscopy (FTIR), Capacitance–voltage measurement (C-V), and effective minority carrier lifetime measurement. Before deposition of the surface passivation layer, the Si wafers were oxidized in a piranha solution (H_2SO_4:H_2O_2=1:4) for 10 minutes followed by oxide removal in a diluted hydrofluoric acid (1wt %) for 1 minute. To

investigate the thermal stability of the stacks, the samples were passed through a standard solar cell contact firing step in a belt furnace with a maximum temperature of 800 °C.

FTIR measurements (Excalibur 3100, Varian) were performed on SiO_yN_x films deposited with varying flow ratio of $R = N_2O/SiH_4$ between 0.44 and 77 and deposition temperature from 130 °C to 400 °C. The reference SiN_x films were also investigated for comparison. In order to obtain total absorption for each bond, the integrated area of the Si–N, Si–O, Si–H, N–H and O–H absorption bands in FTIR was calculated following the procedure of Lanford and Rand [10].

The effective minority carrier lifetime (τ_{eff}) and the fixed charge density Q_f of the films were extracted via corona charge analysis during microwave photo conductance decay (MW-PCD) measurements (WT2000, Semilab). With a white light bias of nearly 1 Sun, the effective carrier lifetime was obtained as a function of the corona charge (Q_c) deposited on the front surface. Since the corona charge was applied only to the front surface, it has no influence on backside surface passivation. The variation of effective minority carrier lifetime can be attributed directly to the change in front surface. We assume that all silicon substrates have the same quality and that carrier generation is uniform in the silicon wafer. Thus, the effective lifetime can be expressed as a function of effective surface recombination velocity S_{eff} [11]

.

$$\frac{1}{\tau_{eff}} \approx \frac{1}{\tau_b} + \frac{2S_{eff}}{W} \qquad Q_c = 0 \qquad (1)$$

$$\frac{1}{\tau_{eff}} \approx \frac{1}{\tau_b} + \frac{S_{front}}{W} + \frac{S_{back}}{W} \qquad \text{When } Q_c \text{ applied} \qquad (2)$$

At the initial state ($Q_c = 0$), $S_{eff} = S_{front,0} = S_{back}$ because the passivation condition on the front and back surface are the same. When combining eq. (1) with eq. (2), the S_{front} at each Q_c can be calculated from the measured lifetime. The surface recombination at the front side reaches a maximum ($S_{front,max}$) at the point where the fixed charge density is totally compensated by the deposited corona charge. Then, field-effect passivation is essentially nullified, and the remaining passivation is chemical

passivation, dominated by D_{it}.

After τ_{eff} measurements, C-V measurements were performed to characterize the interface state density (D_{it}) of single SiN_x layers and SiO_yN_x/SiN_x stacks using a Keithley 4200 SCS. Metal–insulator–semiconductor (MIS) capacitor structures as $Al/SiN_x/SiO_yN_x/Si/Al$ and $Al/SiN_x/Si/Al$ were fabricated using thermal evaporation of Al through a shadow mask. During C-V measurement, the series resistance attributed to either the bulk or the back contact of the silicon wafer could be automatically compensated. Quasi-static C-V measurements on typical SiN_x and SiO_yN_x/SiN_x prepared in this work could not be performed as the films were too leaky. Hence, the absolute value of D_{it} reported in our work should be taken with caution since D_{it} was solely determined by applying the single frequency Hill–Coleman method [12] by combing C-V with conductance-voltage (G-V) results. Nevertheless, we have confidence in the conclusions derived from this study because they rely on trends, rather than absolute values of D_{it}.

Standard industrial solar cells were manufactured on mc-Si wafers (15.6 × 15.6 cm^2) with a base resistivity of 1–5 Ω·cm. Neighboring wafers were used to ensure equal run-to-run material quality. After saw-damage etching (acidic texturing) in a mixed solution of HNO_3 and HF followed by HF/HCl solution cleaning, a phosphorus-doped 80 Ω/□ emitter was formed via $POCl_3$ diffusion in a conventional tube furnace, followed by wet chemical edge isolation and cleaning. These steps were performed in a solar cell mass production line. Thereafter, the front surface passivation layers, either SiO_yN_x/SiN_x stacks or single SiN_x layers, were deposited in the laboratory. During the SiO_yN_x deposition, three different R as 0.44, 0.65 and 1.54 were utilized and their corresponding cells were defined as GP1, GP2 and GP3, respectively. All the SiO_yN_x layers were deposited at 130°C. Five cells were prepared in each group. After ARC deposition, all the wafers were transferred back into the solar cell mass production line, in the same factory, to complete metallization and current–voltage measurement which was performed under the illumination of AM1.5.

PID tests were conducted using a PIDcon instrument (Reiberg Instruments GmbH) through in situ recording of the shunt resistance (R_{sh}) at 60 °C with an applied

negative voltage of 1000 V. A sandwich structure (Glass–EVA–cell–metal plate) without lamination was adopted for the measurements. In this approach, R_{sh} is taken as PID sensitivity because PID usually accompanies R_{sh} degradation and leakage current increase. A detailed description of this method is presented elsewhere [13].

3. Results and Discussion

3.1 Chemical composition

Figure 1 shows the effect of R on the chemical bonds in the deposited SiO_yN_x films via FTIR and reference SiN_x film. The SiN_x films has the largest Si-H and N-H concentration compared to the other SiO_yN_x films, which means the total H concentration is higher than the one in SiO_yN_x films. The Si–O and N–H bond concentration increases as a function of the gas flow ratio as shown in Fig. 1(a). In contrast, the Si–H and Si–N content decreases as the oxygen content in the film increases. In order to illustrate the relative change of various chemical bonds, we plot the [Si-H] / [N-H], and [Si-N] / [Si-O] as function as of R in SiO_yN_x films. As shown in Fig.1 (b), The [Si-H] / [N-H] in SiN_x film is about 0.23, it is very lower than the value in SiO_yN_x films, especially in SiO_yN_x deposited at R <1.0. For SiO_yN_x films, [Si-H] / [N-H], and [Si-N] / [Si-O] both decrease with the increasing of R. This trend is consistent with the anticipated gradual increase in the oxygen concentration in the films. When R rises to 77, the Si-O peak dominates in the FTIR spectrum, while other peaks become negligibly small (not shown here). In this work, this film is defined as SiO_x. During plasma deposition of SiO_yN_x films, the strength of the chemical bonds Si-O and Si-N is 799.6 and 470 kJ/mol, respectively [14]. Therefore, formation of the Si–O bonds is more favorable than the Si-N bonds. When R is higher, the number of SiH_n radicals per O radical decreases, leading to oxygen sufficiency; thus, SiH_n/O reactions can occur leading to more Si–O and O–H in the films [15].

Figure 2.

Figure 2 shows the Si–N, Si–O, N–H, Si–H, and O–H content, as well as the ratio of [Si-H] to [N-H], and [Si-N] to [Si-O], as a function of deposition temperature. When the deposition temperature increases, the Si–O content slightly increases while

the Si–N content remains almost constant. The extent of Si–H, N–H, and O–H bonding decreases as the deposition temperature increases. This behavior is attributable to the film densification through the restructuring of Si–H, N–H, and O-H to form Si–N and Si-O. In addition, the [Si-H] / [N-H], and [Si-N] / [Si-O] ratio both decrease slightly with increasing deposition temperature.

Figure 3.

3.2 Optical properties

In order to apply this surface passivation layer as ARC in solar cells, the optical properties, especially optical refractive index of the SiO_yN_x layer should be investigated. Fig. 3 shows the refractive index of SiO_yN_x layers as a function of flow ratio at different deposition temperature. It can be seen that the refractive index varies from 2.1 to 1.48, when R increases from 0.44 to 77 at a deposition temperature of 300 ^oC. This indicates the films changed from nitride-like to oxide-like when N_2O flow rate increase. The value of 1.48 for pure SiO_x is also consistent with previous reports [16]. The value of n is determined by the composition of the material, and can therefore be related to the bond concentrations Si-N，Si-O, O-H, Si-H and N-H obtained from FTIR. At a constant deposition temperature, the refractive index of SiO_yN_x decreases when R increases, which can be attributed to the increased oxygen content in the films. Thus, the value of n of SiO_yN_x films can be easily controlled by adjusting the N_2O and SiH_4 gas flow. At the same time, the effect of deposition temperature on the value of n also depends on R. When R is 1.54, the n of SiO_yN_x films deposited at 130 ℃ and 300 °C are similar, whereas when R is 0.44, the n is found to be 1.8 and 2.1 for deposition temperatures at 130 °C and 300 °C, respectively. The reason might be that the SiO_yN_x films deposited at high temperature will be denser than deposited at low temperature[17], as indicated in Fig. 2(b).

3.3 Surface passivation

Table I

The effect of annealing upon the values of D_{it} and Q_f resulting from the SiO_yN_x/SiN_x stacked layers was investigated based on their lifetime and chemical structure in our previous reports [18]. Table I presents the difference in D_{it} and fixed

charge density Q_f for representative SiO_yN_x/SiN_x-stack-coated silicon before and after annealing. It is clear that SiO_yN_x/SiN_x stacked layers are stable during high-temperature annealing, which is important for their potential application on crystalline silicon solar cells. The high temperature firing process induces an evident decrease of D_{it} from 1×10^{11} to 1×10^{10} cm^{-2} eV^{-1} for both samples. This could be a reason for the increase in effective lifetime after annealing. Meanwhile, there is a slight decrease in Q_f. The decrease of Q_f and D_{it} after annealing may be attributed to the hydrogen diffused from dielectric films to terminate Si dangling bonds near the interface.

3.3.1 The effect of R and deposition temperature of SiO_yN_x films on stack's surface passivation

Fig. 4 shows a plot of S_{front} as a function of deposited corona charge density for annealed stacks containing SiO_yN_x films deposited at various R and deposition temperature. For single SiN_x and SiO_yN_x films in the stack with less oxygen content, the leakage current in the films induces S_{front} to be almost saturated when the Q_c increases. $S_{front,\,max}$ with a value over 648 cm/s was obtained at a 1 Sun bias light for zero net charge ($Q_f + Q_C = 0$) in the sample coated with single SiN_x layer. However, $S_{front,\,0}$ is less than 100 cm/s for the same sample prior to the deposition of corona charges due to a strong field-effect passivation introduced by the high positive charge. After inserting a thin SiO_yN_x layer between SiN_x and Si substrate, $S_{front,\,0}$ is clearly decreased, indicating improved surface passivation. This surface passivation improvement will degrade when R increases from 0.44 to 1.54. In addition, with the decrease of R, $S_{front,\,max}$ decreases, and the Q_c at the point of $S_{front,\,max}$ gradually shifts to a lower absolute value implying the decrease of Q_f. This implies that D_{it} and Q_f decrease with R. As for the results for the stacks in which SiO_yN_x was deposited at various deposition temperatures with R at 1.54, the results show that $S_{front,\,0}$ increases significantly from 11 to 70 cm/s at an injection level of 1 sun when the deposition temperature increases from 100 °C to 400 °C (Fig. 4 (b)). Better results with lower S_{eff} are obtained when the SiO_yN_x layer is deposited at a lower temperature in the SiO_yN_x/SiN_x stack. With increasing deposition temperature, the Q_c at the point of

$S_{front,\,max}$ shifts toward high negative charge, which implies the increase of positive Q_f. It can be seen that $S_{front,\,max}$ is approximately ten to twenty times larger than $S_{front,\,0}$ in all the samples, which means that Q_f also contributes to a significant field effect passivation.

3.3.2 **Role of surface passivation in the stack**

Figure.5

As discussed above, both the chemical and field effect passivation result from the use of the single SiN_x and the stacks. As shown in Fig. 5 (a), S_{eff} ($S_{front,\,0}$) depends strongly on D_{it} in the SiO_yN_x/SiN_x stacks. The relation of D_{it} to R and deposition temperature agree with the relation of $S_{front,\,max}$ as shown in Fig.4. As for the stacks, both Q_f and D_{it} increase as the deposition temperature and R increases. As D_{it} increases over one order of magnitude, S_{eff} increases a few times. However, for the single SiN_x and SiO_x/SiN_x stack, the points follow the curve of S_{eff} versus D_{it} in SiO_yN_x/SiN_x stacks. It is surprising that S_{eff} shows a similar relationship with Q_f as with D_{it} in the SiO_yN_x/SiN_x stacks when SiO_yN_x is altered by varying different deposition parameters. As is evident in Fig. 5 (b), $S_{front,\,0}$ increases gradually from 10 cm/s to 70 cm/s as Q_f increases slightly from 6.3×10^{11} cm^{-2} to 1.3×10^{12} cm^{-2}. Regarding the variation in the SiO_yN_x/SiN_x stacks with different SiO_yN_x stoichiometry, we observe that as long as the field effect passivation is sufficient, the D_{it} appears to be a key factor for surface passivation of silicon substrate. For example, in the SiO_yN_x/SiN_x stack structures when Q_f gradually increases, the surface passivation still degrades because of the simultaneous increase in D_{it}. The chemical passivation plays a major role explaining that even though the SiN_x film has the largest Q_f, the value of $S_{front,0}$ is 56 cm/s, far larger than that of SiO_yN_x/SiN_x-stacked layers after annealing.

Figure. 6

[Si–H] is regularly considered as a measure of surface passivation quality for SiN_x passivation layer owing to the hypothesis that higher [Si–H] implies a higher probability that hydrogen terminates the Si dangling bonds at the SiN_x - Si interface[19]. Moreover, the lowest value of D_{it} was obtained in Si-rich SiN_x with highest Si-H and lowest N-H bond [20]. In order to clarify the dependence of Q_f and D_{it} on Si –H and

N-H, we plot D_{it} and Q_f of SiO_yN_x/SiN_x stacks as a function of [Si-H] / [N-H] in SiO_yN_x films deposited at various R, deposition temperature (Fig. 6). The result of single SiN_x films is shown as comparison. The data indicates that D_{it} and Q_f are strongly influenced by the [Si-H] / [N-H] for stacks and single SiN_x. They decrease with the increase of [Si-H] / [N-H] from the point of SiN_x. This indicates the [Si-H] / [N-H] ratio has the same influence on D_{it} and Q_f for the SiO_yN_x/SiN_x stacks and single SiN_x film. Also, it shows that low deposition temperature during deposition of SiO_yN_x will induce high [Si-H] / [N-H] in the SiO_yN_x film, low Q_f and D_{it} in the stack. In addition, combined with the result in Fig. 1, Fig. 2 and Fig. 6, it also can be shown the D_{it} and Q_f for the stacks decrease with the increase of [Si-N]/[Si-O] in SiO_yN_x films. However it is not easy to see a correlation between D_{it}, Q_f and Si-N for both single SiN_x film and SiO_yN_x/SiN_x stacks, because the former has the biggest [Si-N], but the highest D_{it} and Q_f. This might indicate that [Si-N] is not the reason that induce the difference of performance on Q_f and D_{it} between single SiN_x and the stack, even though in SiN_x layer, the [Si-N] has been thought the main influence factor on the surface passivation on silicon [21, 22]. This further indicates that in both SiO_yN_x/SiN_x stacks and single SiN_x films, the main affecting factor to D_{it} and Q_f is the ratio of [Si-H] / [N-H]. The increase of N and O radicals and deposition temperature can help more Si to bond with oxygen and the N–H bond increases while the Si–H fraction decreases. On the other hand, the decrease in the N and O radicals in the plasma can improve the interaction with the SiH_n radicals. This can be in favor of Si–H formation and reduce the positive charged defects formation in the SiO_yN_x films, such as N≡Si, N_2O≡Si, NO_2≡Si, and O≡Si, et al. [23]. Furthermore, the increased Si–H bonds at the interface suppress the formation of the interface state and improve the H passivation of the Si dangling bonds at the interface. In short, inserting a thin SiO_yN_x layer can decrease the N-H and increase Si-H contents at the interface, resulting in a superior chemical passivation.

3.3.3 The optimal of SiO_yN_x films for stack's surface passivation

An extended temperature range of 35 °C–400 °C at the optimal flow ratio of 0.44 was employed to further investigate the effect of SiO_yN_x deposition temperature. As

shown in Fig. 7, for as-deposited SiO_yN_x/SiN_x stack, the S_{eff} decreases from 13 to 10 cm/s when the SiO_yN_x deposition temperature increases from 35 °C to 130 °C. After firing, the S_{eff} decreases 3-fold compared to that of as-deposited stacks. The relation between S_{eff} and the SiO_yN_x deposition temperature is the same for samples before and after annealing. This further verifies that the SiO_yN_x/SiN stack has a good thermal stability. The best surface passivation was achieved in samples deposited at temperatures of 100 °C to 200 °C with S_{eff} in a range of 2–3 cm/s after firing. However, S_{eff} of the stack passivated samples where SiO_yN_x is deposited outside the temperature range of 100 °C–200 °C still remains below 10 cm/s, as shown in Figure 7.

Figure 8.

For the stack structure we find that both the flow ratio and the deposition temperature used for the SiO_yN_x layer has a substantial effect on the passivation quality. However, the thickness of SiO_yN_x in the stack structure might also affect the passivation quality. The effect of SiO_yN_x thickness in the SiO_yN_x/SiN_x-stacked layers, on the passivation quality is shown in Fig. 8. The S_{eff} for the samples with SiO_yN_x/SiN_x stack is in the range of 1.8 ~ 3.2 cm/s as the SiO_yN_x thickness varied from 2 to 50 nm. Furthermore, the best value of 1.8 cm/s is obtained when the SiO_yN_x layer thickness is 6 nm.

3.4 Solar cell results

Based on the results described above, a stack layer was selected for application to industrial mc-Si solar cells. The selected stack is a SiO_yN_x (10nm)/SiN_x (70nm, n=2.04) stacks. The reference single SiN_x layers was 80 nm with n=2.04. The value of n of the SiO_yN_x layer for GP1 (R=0.44), GP2 (R=0.65) and GP3 (R=1.54) was 1.8, 1.65, and 1.52, respectively. The weighted average reflectance of the ARC layers with single SiN_x coating and SiO_yN_x/SiN_x stacks were 11.4 % and 10.7-10.9% respectively. Since the SiO_yN_x layer is only 10 nm, the difference in reflectance between GP1, 2 and 3 is very small.

Table II shows the electrical performance of the solar cells incorporating the SiO_yN_x/SiN_x stacks and single-layer SiN_x. The average conversion efficiency of the

solar cells in GP1, 2 and3 varied from 17.6±0.2% to 17.9±0.1%, depending on the SiO_yN_x film deposition process. As a reference, the traditional structure with single-layer SiN_x coating resulted in an average conversion efficiency of only 17.4±0.1%. A full 0.5% absolute increase was gained on the average conversion efficiency for the best SiO_yN_x/ SiN_x-coated mc-Si solar cells (GP1, GP2) compared to the reference cells. For samples in GP1-3 coated with SiO_yN_x/SiN_x stacks, the short-circuit current I_{sc} was slightly increased. The open-circuit voltage (V_{oc}) as well as the fill factor (FF) increases significantly compared to the reference cells for GP1 and GP 2, where the SiO_yN_x layer was deposited at small R, which is consistent with the τ_{eff} results. The increase of I_{sc} can be attributed to the better optical absorption due to lower reflection. The improvement of solar cell performance, especially V_{oc} and FF is mainly attributed to the improved surface passivation which reduces the saturation current density on the emitter.

Table II

Figure 9.

To investigate the PID behavior of the mc-Si solar cells, a sensitivity analysis of PID on non-encapsulated silicon solar cells was conducted. The R_{sh} during the PID testing is plotted in Fig. 9. All the cells with SiO_yN_x/SiN_x stacks show stable R_{sh} during the PID testing except the samples in group GP3, which revealed a small degree of degradation (5%) after 24 hours. However, the single SiN_x-coated silicon solar cell shows a significant degradation (>50%) after 24 hours. These results show that the insertion of a thin SiO_yN_x layer beneath the SiN_x layer significantly improves the resistance to PID. However, the improvement on the PID-resistance also depends on the composition of SiO_yN_x layer, varied by deposition condition as R.

Conventional characterization of current–voltage (I-V) curve [24] was employed on the dielectric film to find the reason for the solar cell PID resistance improvement. Our I–V of the dielectric film results revealed that after insertion of a SiO_yN_x layer between SiN_x and Si, the electrical insulation of the ARC was enhanced [8]. This might indicate that the conductivity of the dielectric layers does not provide a reasonable explanation for the excellent PID resistance for the SiO_yN_x/SiN_x stack

coated silicon solar cells. In this paper, compared with single SiN_x coated solar cells, the introduced Si–O bonds have effectively inhibited the occurrence of PID. However, it was reported the increase of Si–O when R increases during the SiO_yN_x deposition can also slightly degrade R_{sh} because a high oxygen content in the SiN_x thin film will result in electrochemical corrosion of the dielectric film, thus increasing the PID [25]. When considering the result of chemical composition (as shown in Fig. 1), it is also important that the rise of the PID correlates with an increase in the concentration of N–H bonds. It has been proposed that the quality of the dielectric/Si interface could be a key factor for PID [28]. Then we conclude the concentration of N-H at the interface may affect the damage caused by voltage stress at the SiO_yN_x/Si and SiN_x/Si interface, which degrades the surface passivation and increases the leakage current of the solar cells.

4. CONCLUSIONS

In this paper, we systematically studied various deposition conditions for SiO_yN_x films that have been inserted between the Si and the traditional SiN_x capping layer. The composition, refractive index of the films as well, the passivation properties and its effect upon solar cell performance were investigated. It was determined that the N/O composition in SiO_yN_x can be adjusted by changing R as well as the deposition temperature. The n of SiO_yN_x can be adjusted from 1.48 to 2.1 as the R is varied from 77 to 0.44. As R is decreased from 77 to 0.44, D_{it} decreased from 4.50×10^{11} cm^{-2} eV^{-1} to 3.96×10^{10} cm^{-2} eV^{-1} resulting in a good surface passivation with low S_{eff}. Compared to SiN_x passivation layer, in the SiO_yN_x/SiN_x stacks, the decrease of N-H bonds and increased Si-H bond can be the reason for improved surface passivation. The deposition temperature had a slight effect on the N/O composition in the SiO_yN_x films as well as the passivation quality. The optimal SiO_yN_x deposition temperature was found to be 130 °C. However, the samples deposited at other temperatures, the S_{eff} values are still below 10 cm/s. Furthermore, the SiO_yN_x thickness in the stack is not critical to passivation quality. A 6-nm-thick SiO_yN_x in the stack is enough to ensure excellent surface passivation with S_{eff} < 2 cm/s on a 1 - 3 Ω·cm FZ planar

p-type Si.

The SiO_yN_x/SiN_x stack has an excellent thermal stability. When it was applied on mc-Si solar cells as a replacement of a single SiN_x coating as ARC, the electrical performance of the solar cells improved significantly. The improvement on V_{oc} and FF is caused by the improved surface passivation which induces a decrease of saturation current density. A maximum absolute efficiency gain of 0.5% was obtained compared to single SiN_x-coated mc-Si solar cells. In addition, resistance to PID is also significantly improved. The stack coated solar cells only degraded at most 5% and some cells even exhibited nearly zero degradation in R_{sh} after 24 hours in the PID testing. However, the single-layer SiN_x-coated silicon solar cell showed substantial degradation in R_{sh} with over 50% after 24 hours in the same test. The N-H bonds, or [Si-H] / [N-H] in the dielectric layers were found to play a major role for resistance of PID.

Acknowledgements

The financial support from the research project 221668/E20, 193829/E20 granted by Norwegian Research Council is gratefully acknowledged. The authors would also like to thank the National High Technology Research and Development Program of China for financial support under grant No. 2015AA050302.

REFERENCES

[1] A. del Prado, E. San Andrés, F.L. MartÍnez, I. Mártil, G. González-DÍaz, W. Bohne, et al. Composition and optical properties of silicon oxynitride films deposited by electron cyclotron resonance. Vacuum 2002;67:507-512.

[2] J Dupuis, E Fourmond, JF Lelievre, D Ballutaud, M Lemiti. Impact of PECVD SiON stoichiometry and post-annealing on the silicon surface passivation. Thin Solid Films. 2008; 516:6954-6958.

[3] J. Seiffe, L. Gautero, M. Hofmann, J. Rentsch, R. Preu, S. Weber, et al. Surface passivation of crystalline silicon by plasma-enhanced chemical vapor deposition double layers of silicon-rich silicon oxynitride and silicon nitride. J Appl Phys. 2011;109:034105.

[4] J. Seiffe, L. Weiss, M. Hofmann, L. Gautero, J. Rentsch. Alternative Rear Surface Passivation for Industrial Cell Production. 23rd European Photovoltaic Solar Energy Conference Valencia, Spain 2008.

[5] A. Laades, M. Blech, H. C. Biank, C. Maier, Maurizio Roczen, C. Leschinski, et al. Fudamental Study of Silicon Oxynitrides for Photovoltaic Applications. 26th European Photovoltaic Solar Energy Conference and Exhibition. Hamburg, Germany2011.

[6] Brett Hallam, BudiTjahjono, StuartWenham Effect of PECVD silicon oxynitride film composition

on the surface passivation of silicon wafers. Solar Energy Materials&Solar Cells 2012;96:173-179.
[7] Lu Wang, Anthony Lochtefeld, Jianshu Han, Andrew P. Gerger, Mark Carroll, Jingjia Ji, et al. Development of a 16.8% Efficient 18-μm Silicon Solar Cell on Steel. IEEE JOURNAL OF PHOTOVOLTAICS. 2014;4:1397-1404.
[8] Chunlan Zhou, Junjie Zhu, Sean E. Foss, Halvard Haug, Ørnulf Nordseth, Erik S. Marstein, et al. SiOxNy/SiNx Stack Anti-reflection Coating with PID-resistance for Crystalline Silicon Solar Cells. 5th International Conference on Silicon Photovoltaics, SiliconPV 2015. Konstanz, Germany, 2015.
[9] D. N. Wright, E.V. Monakhov, E.S. Marstein, A.Yu. Kuznetsov, B.G. Svensson, and A. Holt. The Effect on Surface Passivation of the Deposition Power in Plasma Enhanced Chemical Vapour Deposition Silicon Nitride. 21st European Photovoltaic Solar Energy Conference and Exhibition. Dresden, Germany, 2006.
[10] W. A. Lanford and M. J. Rand. The hydrogen content of plasma‐deposited silicon nitride. J Appl Phys. 1978; 49: 2473.
[11] A. Cuevas, D. Macdonald. Measuring and interpreting the lifetime of silicon wafers. Solar Energy Materials & Solar Cells. 2004;76 255-262.
[12] W. A. Hill and C. C. Coleman. A single-frequency approximation for interface-state density determination. Solid-State Electronics. 1980;23:987-993.
[13] Dominik Lausch, Volker Naumann, Otwin Breitenstein, Jan Bauer, Andreas Graff, J¨oerg Bagdahn, et al. Potential-Induced Degradation (PID): Introduction of a Novel Test Approach and Explanation of Increased Depletion Region Recombination. IEEE JOURNAL OF PHOTOVOLTAICS MAY 2014; 4:834-40.
[14] D.R. Lide. Handbook of Chemistry and Physics: CRC Press LLC,New York; 2004.
[15] M.I. Alayo, I. Pereyra, W.L. Scopel, Fantini MCA. On the nitrogen and oxygen incorporation in plasma-enhanced chemical vapor deposition (PECVD) SiOxNy films. Thin Solid Films. 2002;402:154–161.
[16] Sinje Keipert-Colberg, Nadine Barkmann, Christian Streich, Andreas Schütt, Dominik Suwito, Petra Schäfer, et al. Investigation of a PECVD silicon oxide/silicon nitride passivation system concerning process influences. 26th European PV Solar Energy Conference and Exhibition Hamburg, Germany, 2011.
[17] J. Kanicki. Roll of Hydrogen in Silicon Nitride Films Prepared by Various Deposition Techniques. Mat Res Soc Symp Proc,. 1988;118: 671-677.
[18] J.J Zhu, S. Zhou, H. Haug, E.S. Stensrud Marstein, S.E. Foss, W.J. Wang. A Firing Stable Passivation for P-type Si substrate. 29th European Photovoltaic Solar Energy Conference and Exhibition. Frankfurt, Germany 2014.
[19] H. M¨ackel and R. L¨udemann. Detailed study of the composition of hydrogenated SiN x layers for high-quality silicon surface passivation. Journal of Applied Physics. 2002; **92**: 2602-0609.
[20] Stefaan De Wolf, Guido Agostinell, Guy Beaucarne, Petko Vitanov. Influence of stoichiometry of direct plasma-enhanced chemical vapor deposited SiN_x films and silicon substrate surface roughness on surface passivation. J Appl Phys 2005;97:063303.
[21] A.W. Weeber, H.C. Rieffe, I.G. Romijn, W.C. Sinke, Soppe WJ. The Fundamental Properties Of SiN_x:H That Determine Its Passivating Qualities. 31st IEEE PVSC. 2005:1043 -1046.
[22] Yimao Wan, Keith R. McIntosh, Thomson aAF. Characterisation and optimisation of PECVD SiNx as an antireflection coating and passivation layer for silicon solar cells. AIP ADVANCES.

2013;3:032113.
[23] A.G. Aberle. Overview on SiN surface passivation of crystalline silicon solar cells. Solar Energy Materials and Solar Cells 2001;65:239-248.
[24] V. Naumann, K. Llse, C.Hagendorf. On the Discrepancy between Leakage Currents and Potential-Induced Degradation of Crystalline Silicon Modules. Proceedings of 28th European Photovoltaic Solar Energy Conference and Exhibition. Paris, France 2013. p. 2994-2997.
[25] Ken Mishina, Atsufumi Ogishi, Kiyoshi Ueno, Takuya Doi, Kohjiro Hara, Norihiro Ikeno, et al. Investigation on antireflection coating for high resistance to potential-induced degradation. Jpn J Appl Phys 2014;53:03CE1.
[26] D. R. Lee, C. Parker, J. R. Hauser, and G.Lucovsky. Reliability of nitrided Si–SiO_2 interfaces formed by a new, low‐temperature, remote‐plasma process. J Vac Sci TechnolB. 1995;13:1788-1793.
[27] G. Lucovsky, Z. Jing aDRL. Defect properties of Si, O, N, and Hatoms at Si—SiO2 interfaces. J Vac Sci Technol B 1996;14:2832-2839.
[28] Nitsa Kindyni, and George E. Georghiou. Description and Analysis of Potential Induced Degradation in Crystalline Silicon Solar Cells and Modules Based on Transistor Principles. 27th European Photovoltaic Solar Energy Conference and Exhibition. Frankfurt, Germany 2012.

Table I. The D_{it} and fixed charge Q_f difference before and after annealing for SiO_yN_x/SiN_x stack coated silicon.

Sample		D_{it} ($cm^{-2}eV^{-1}$)	Q_f (cm^{-2})
A($n_{SiO_xN_y}$=1.93)	as-deposited	1.26×10^{11}	1.58×10^{12}
	after firing	1.24×10^{10}	1.09×10^{12}
B($n_{SiO_xN_y}$=1.59)	as-deposited	1.85×10^{11}	1.72×10^{12}
	after firing	2.24×10^{10}	1.22×10^{12}

Table II. The effect of R on electrical performance for SiO_yN_x/SiN_x stacks and single SiN_x coated mc-Si solar cells. The results were the average value of 5 cells in each group.

Sample	V_{oc} **(mV)**	I_{sc} **(A)**	***FF*** **(%)**	η **(%)**
Reference: SiN_x only	627±1	8.51±0.02	79.44±0.05	17.4±0.1
GP1: SiO_yN_x/SiN_x SiO_yN_x：R=0.44	633±1	8.58±0.03	80.04±0.02	17.9±0.1
Gp2: SiO_yN_x/SiN_x SiO_yN_x：R=0.65	633±1	8.55±0.05	80.23±0.19	17.9±0.1
GP3: SiO_yN_x/SiN_x SiO_yN_x：R=1.54	630±2	8.56±0.02	79.61±0.28	17.6±0.2

Figure captions

Figure 1. The effect of precursor ratio R on the chemical bonds in SiO_yN_x films. (a) The absorption intensity of chemical bonds in SiO_yN_x films from FTIR measurements; (b) the ratio of [Si-H] to [N-H], and [Si-N] to [Si-O]. The data come from the fired sample.

Figure 2. Chemical bonds calculated from FTIR measurements for SiO_yN_x films deposited at variable temperature. (a) The total chemical bonds absorption for Si-N, Si-O, Si-H, N-H, O-H in SiO_yN_x films; and (b) the ratio of [Si-H] to [N-H], and [Si-N] to [Si-O]. The data come from the fired sample.

Figure 3. The function of optical refractive index with R during SiO_yN_x deposition at deposition temperature of 130 and 300 ^oC respectively. The data come from the fired sample.

Figure 4. Surface recombination velocity at front side S_{front} for the SiO_yN_x (30 nm)/SiN_x (n=2.04, 70 nm) stack measured at an injection density of 1 sun as a function of deposited Corona charge density $Q_{c.}$ (a) the SiO_yN_x films was deposited at 300^{o}C with different R and (b) at different deposition temperature. The 100 nm single SiN_x films presents as a reference. The data come from the fired sample.

Figure 5. (a) Extracted S_{eff} ($S_{front,\ 0}$) from corona charge effective minority carrier lifetime measurement are plotted as a function of (a) interface density D_{it} at midgap and (b) fixed charge Q_f for the SiO_yN_x (30 nm)/SiN_x (n=2.04, 70 nm) stack -passivated silicon wafer for SiO_yN_x in the stacks deposited at various R, deposition temperature. The 100 nm single SiN_x films and SiO_x/SiN_x present as a comparison.

Figure 6. Interface density D_{it} at midgap, and fixed charge Q_f in the SiO_yN_x (30 nm)/SiN_x (n=2.04, 70 nm) stack as a function of Si-H/N-H for SiO_yN_x deposited at a various conditions, (a) R and (b) deposition temperature. The arrow of "N_2O/SiH_4 flow rate" and "deposition temperature" show the value for "N_2O/SiH_4 flow rate" and "deposition temperature" are increase from right to left along the top X axis.

Figure 7. The effect of deposition temperature on S_{eff} for SiO_yN_x (30nm)/SiN_x (n=2.04, 70nm) coated planar silicon wafer with SiO_yN_x deposited at R=0.44. The data come from the fired sample.

Figure 8. The effect of SiO_yN_x thickness on S_{eff} for SiO_yN_x/SiN_x (n=2.04, 70nm) coated planar silicon wafer with SiO_yN_x deposited at R=0.44. The data come from the fired sample.

Figure 9. PID test results; normalized R_{sh} as a function of PID testing time.

Fig .1

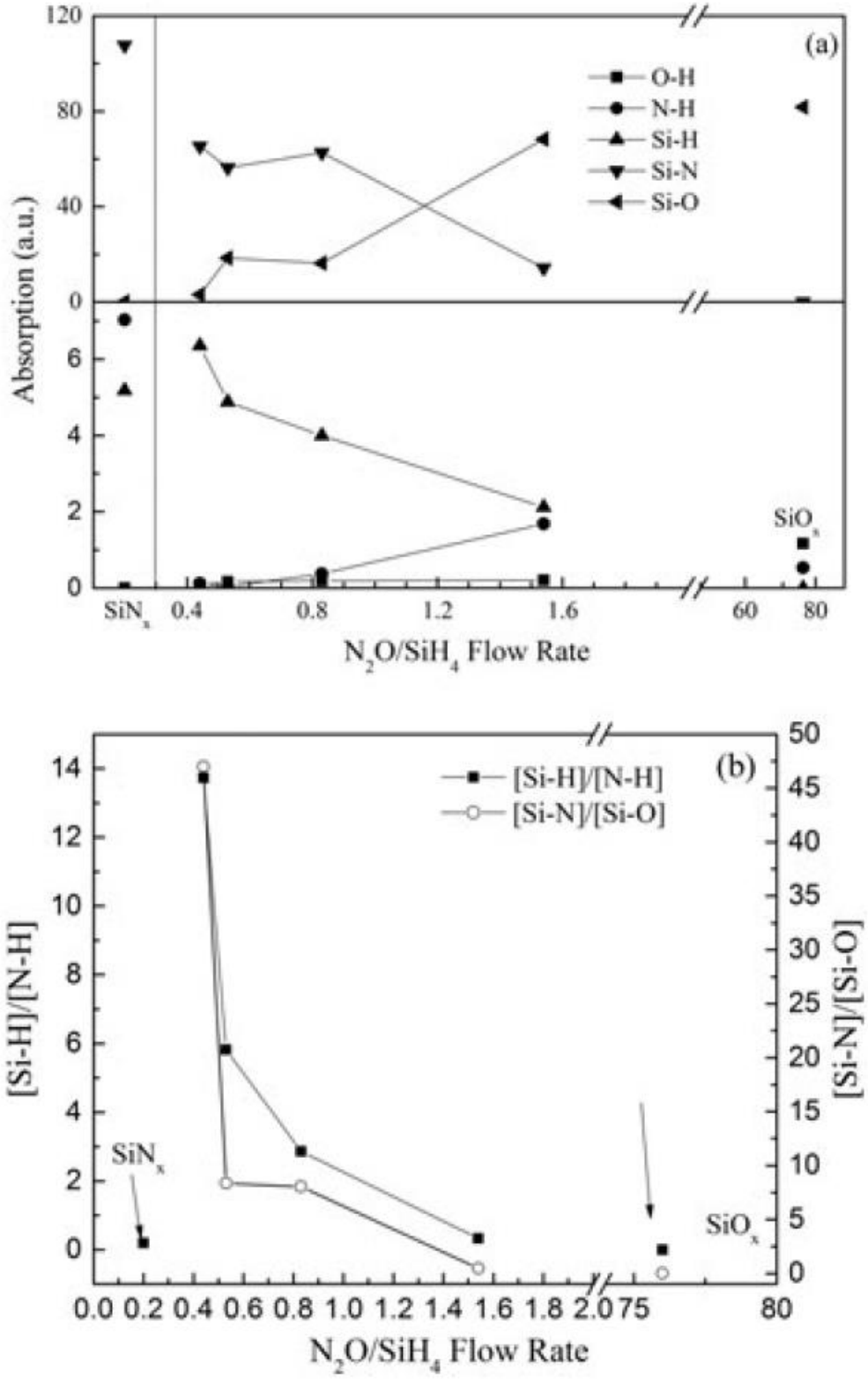
(a)
O-H
N-H
Si-H
Si-N
Si-O
Absorption (a.u.)
SiN$_x$
SiO$_x$
N$_2$O/SiH$_4$ Flow Rate
(b)
[Si-H]/[N-H]
[Si-N]/[Si-O]
SiN$_x$
SiO$_x$
N$_2$O/SiH$_4$ Flow Rate

Fig. 2

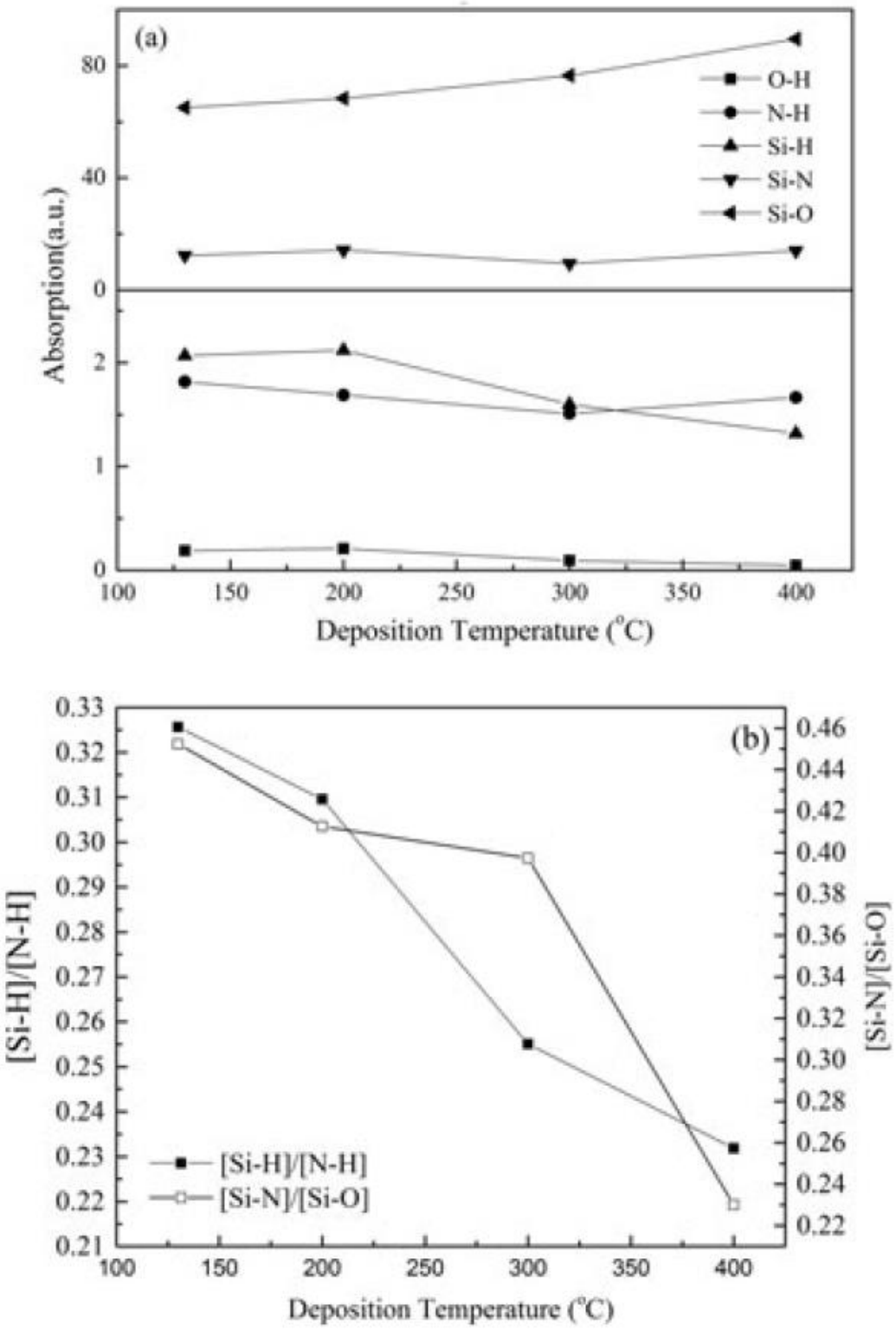
(a)
O-H
N-H
Si-H
Si-N
Si-O
Absorption(a.u.)
Deposition Temperature (°C)
(b)
[Si-H]/[N-H]
[Si-N]/[Si-O]
Deposition Temperature (°C)

Fig.3

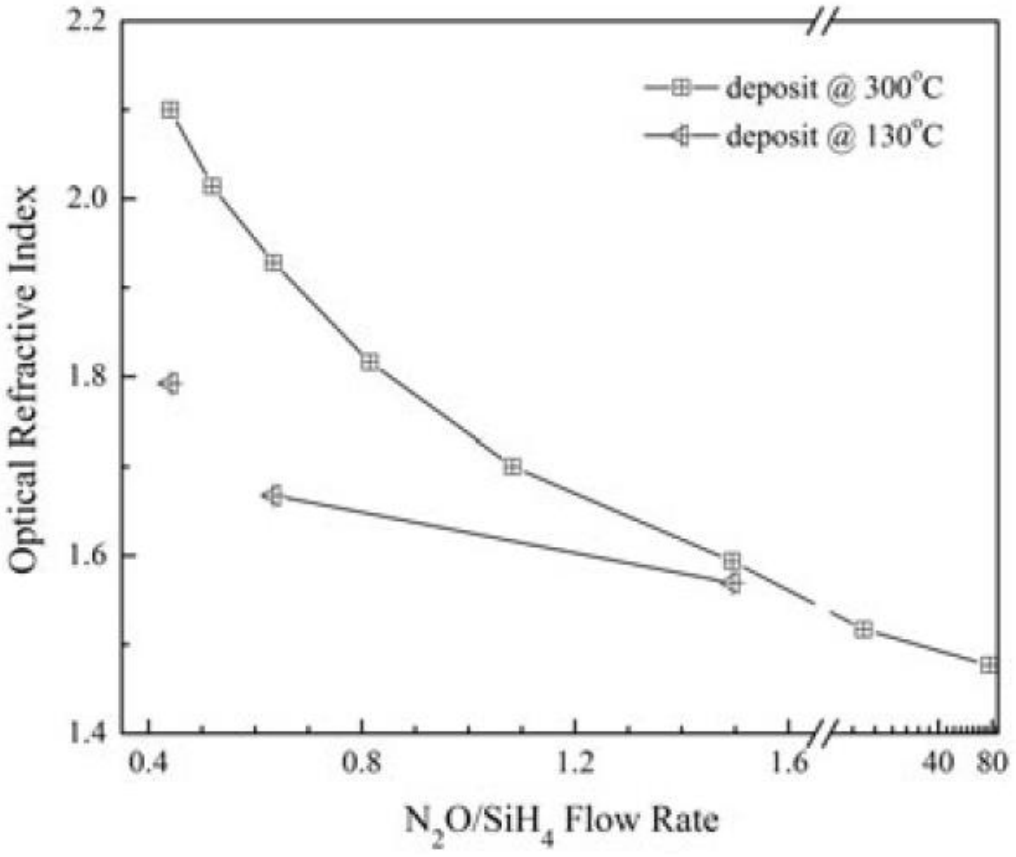
deposit @ 300°C
deposit @ 130°C
Optical Refractive Index
2.2
2.0
1.8
1.6
1.4
0.4
0.8
1.2
1.6
40
80
N2O/SiH4 Flow Rate

Fig.4

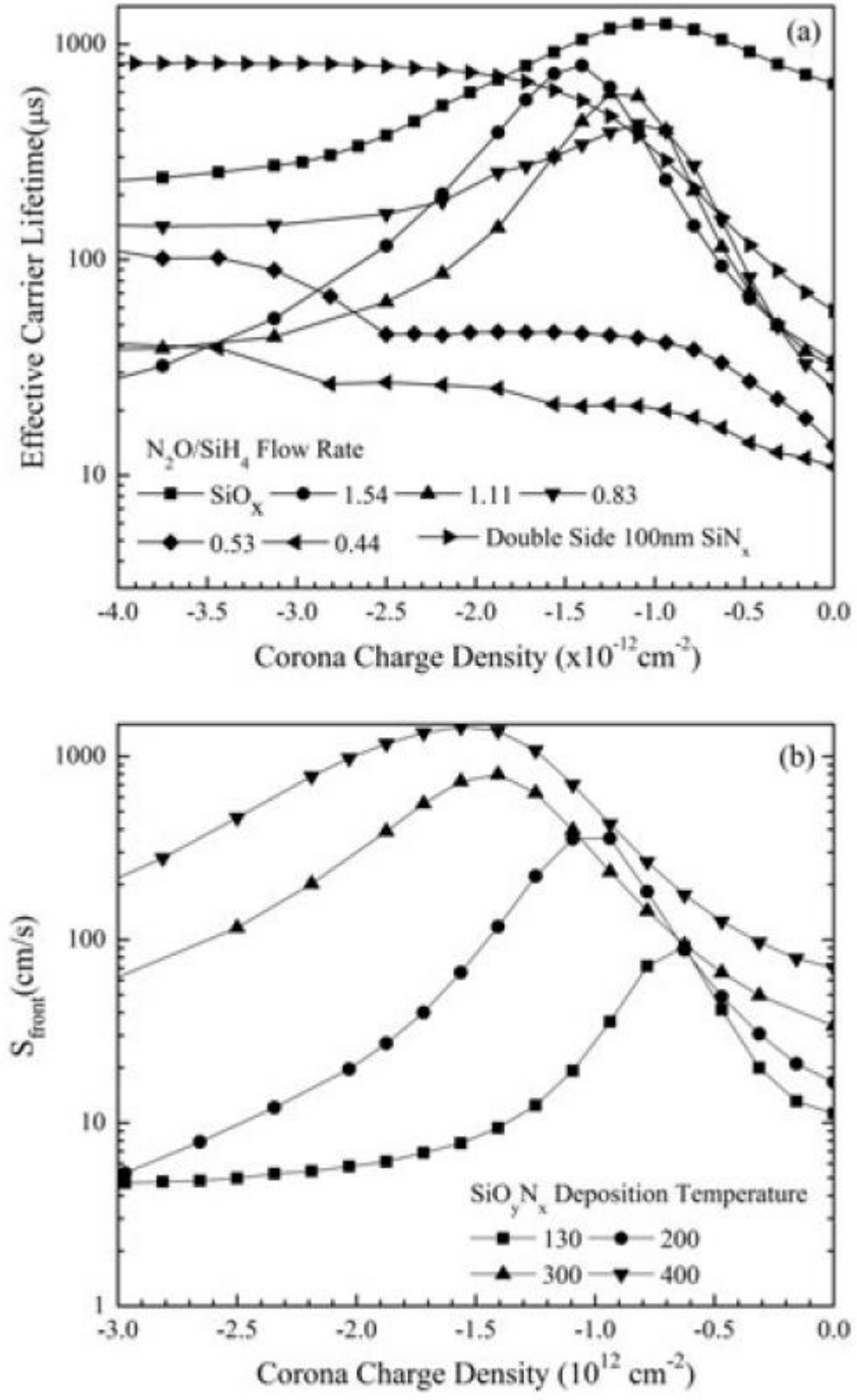
(a)
Effective Carrier Lifetime(μs)
1000
100
10
N2O/SiH4 Flow Rate
SiOX
1.54
1.11
0.83
0.53
0.44
Double Side 100nm SiNx
-4.0
-3.5
-3.0
-2.5
-2.0
-1.5
-1.0
-0.5
0.0
Corona Charge Density (x10-12cm-2)
(b)
Sfront(cm/s)
1000
100
10
1
SiOyNx Deposition Temperature
130
200
300
400
-3.0
-2.5
-2.0
-1.5
-1.0
-0.5
0.0
Corona Charge Density (1012 cm-2)

Fig. 5

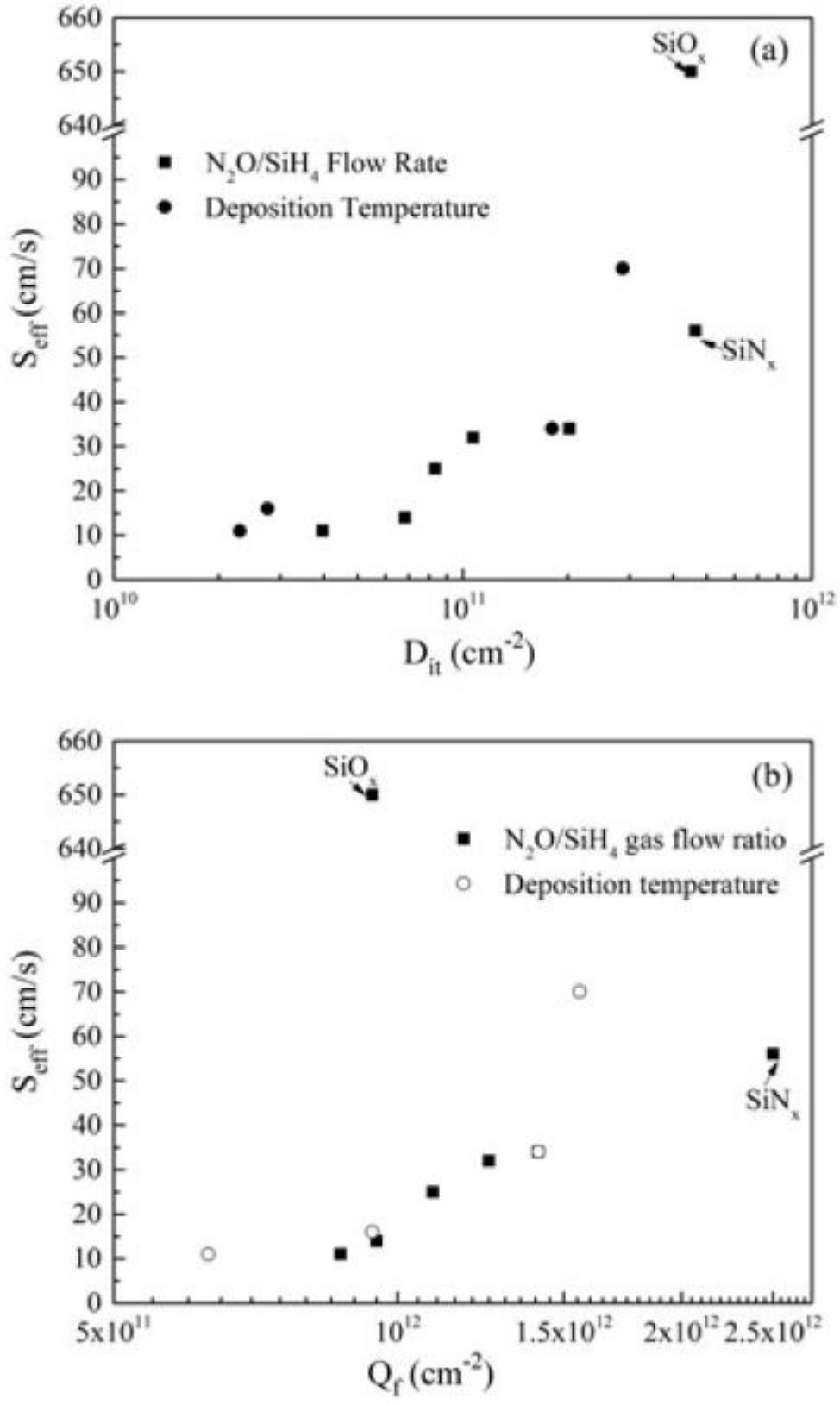
660
650
640
90
80
70
60
50
40
30
20
10
0
SiO$_x$
(a)
N$_2$O/SiH$_4$ Flow Rate
Deposition Temperature
SiN$_x$
S$_{eff}$ (cm/s)
10^{10}
10^{11}
10^{12}
D$_{it}$ (cm^{-2})
SiO$_x$
(b)
N$_2$O/SiH$_4$ gas flow ratio
Deposition temperature
SiN$_x$
5x10^{11}
10^{12}
1.5x10^{12}
2x10^{12}
2.5x10^{12}
Q$_f$ (cm^{-2})

Fig. 6

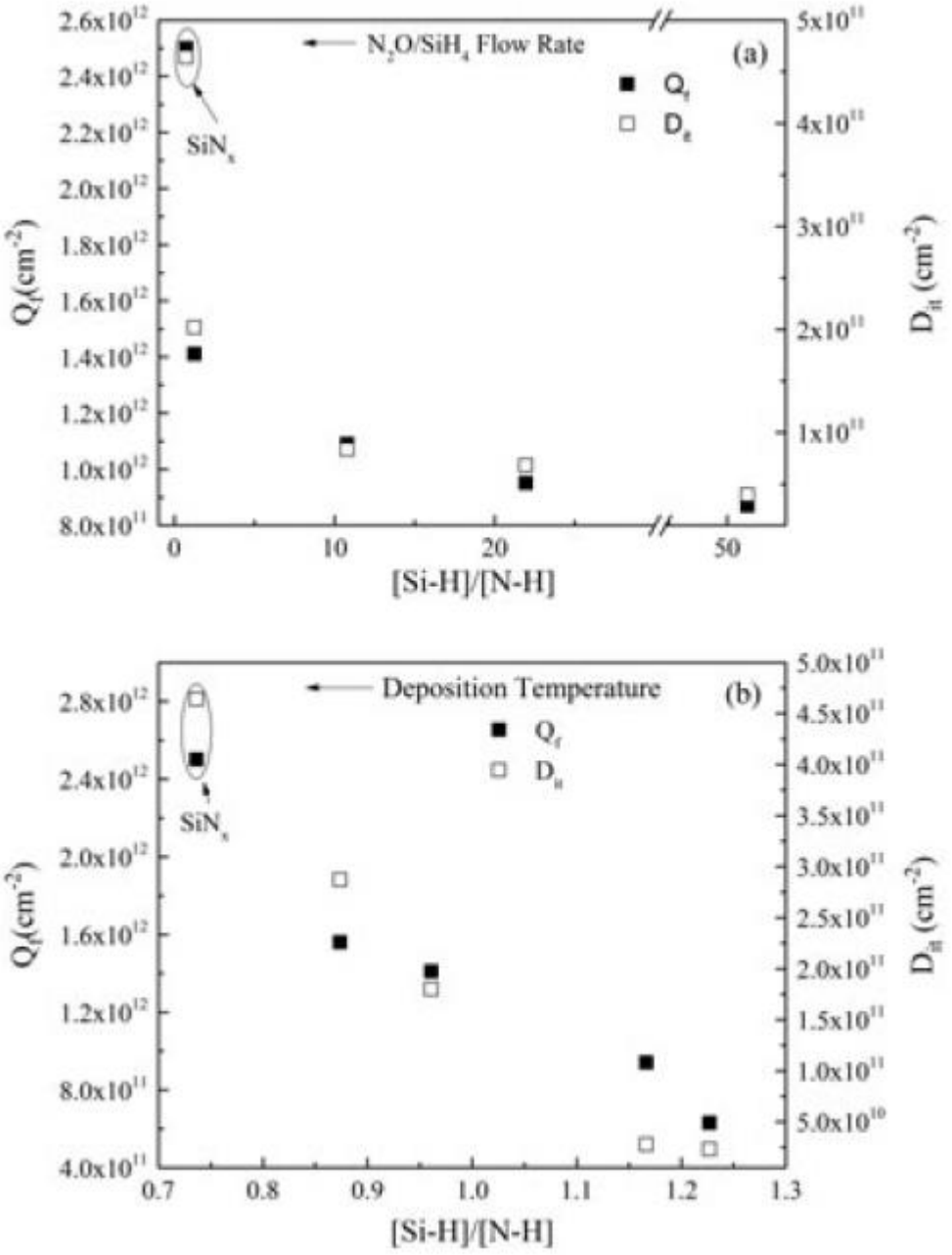
N2O/SiH4 Flow Rate
(a)
Qf
Dit
SiNx
Qf(cm-2)
Dit (cm-2)
[Si-H]/[N-H]
Deposition Temperature
(b)
Qf
Dit
SiNx
Qf(cm-2)
Dit (cm-2)
[Si-H]/[N-H]

Fig. 7

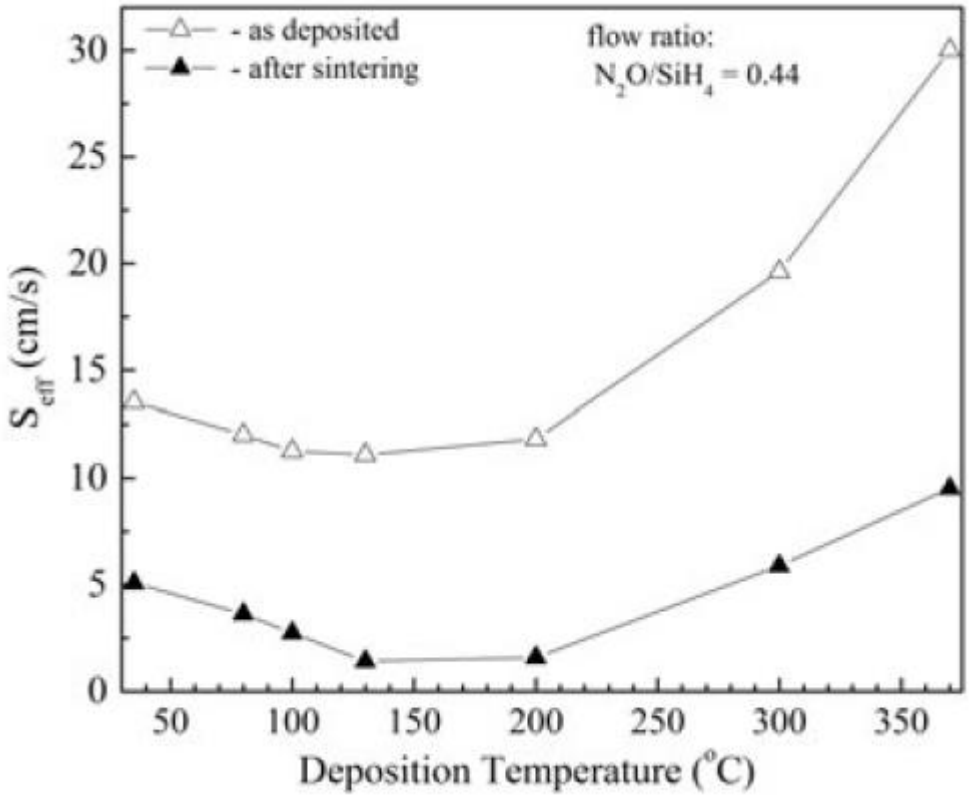
- as deposited
- after sintering
flow ratio:
N2O/SiH4 = 0.44
Seff (cm/s)
0
5
10
15
20
25
30
50
100
150
200
250
300
350
Deposition Temperature (°C)

Fig.8

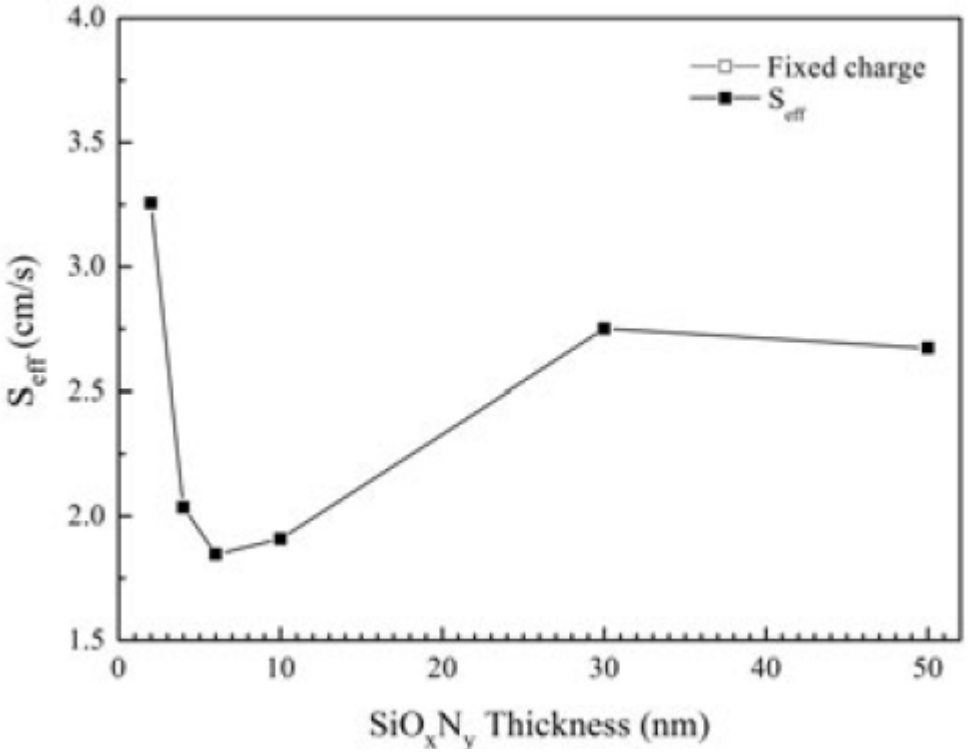
Fixed charge
S_{eff}
S_{eff} (cm/s)
SiO_xN_y Thickness (nm)
4.0
3.5
3.0
2.5
2.0
1.5
0
10
20
30
40
50

Fig.9

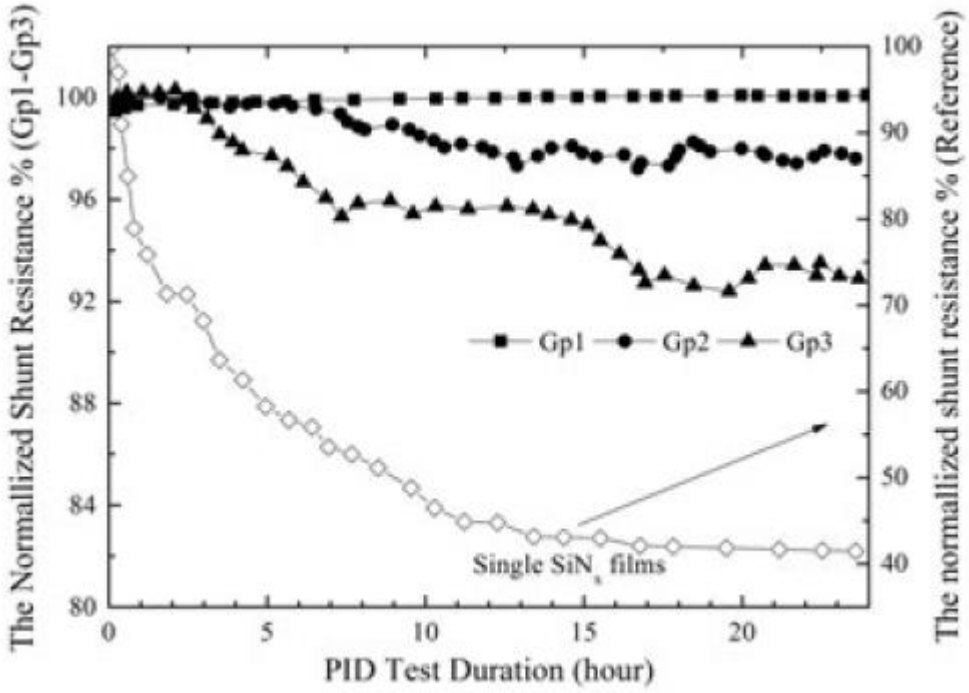
The Normallized Shunt Resistance % (Gp1-Gp3)
The normallized shunt resistance % (Reference)
PID Test Duration (hour)
Gp1
Gp2
Gp3
Single SiNx films
100
96
92
88
84
80
90
70
60
50
40
0
5
10
15
20